



Cite this: *Chem. Commun.*, 2024, 60, 843

Received 13th October 2023,  
Accepted 13th December 2023

DOI: 10.1039/d3cc04982e

rsc.li/chemcomm

# Visible-light-induced ATRP under high-pressure: synthesis of ultra-high-molecular-weight polymers†

Roksana Bernat,<sup>ab</sup> Grzegorz Szczepaniak,<sup>de</sup> Kamil Kamiński,<sup>ab</sup>  
Marian Paluch,<sup>ab</sup> Krzysztof Matyjaszewski<sup>id</sup>\*<sup>d</sup> and Paulina Maksym<sup>id</sup>\*<sup>bf</sup>

**In this study, a high-pressure-assisted photoinduced atom transfer radical polymerization ( $p \leq 250$  MPa) enabled the synthesis of ultra-high-molecular-weight polymers (UHMWPs) of up to 9 350 000 and low/moderate dispersity ( $1.10 < \bar{D} < 1.46$ ) in a co-solvent system (water/DMSO), without reaction mixture deoxygenation.**

Atom transfer radical polymerization (ATRP), since its discovery in the 1990s, has evolved into a powerful synthetic technique.<sup>1</sup> This progress can be attributed to three main factors: the development of new catalysts, the adoption of water as the reaction medium and the use of external stimuli such as light, electrical current and mechanical forces to mediate ATRP.<sup>2–5</sup> Utilizing light has given polymer chemists superior control over polymer growth and characteristics.<sup>6–10</sup> Moreover, using water as a sustainable reaction medium not only reduced the environmental impact of ATRP but also expanded its versatility.<sup>11–15</sup> This advancement enables the synthesis of well-defined polymers with complex structures, like protein–polymers and nucleic acid–polymer hybrids.<sup>16–18</sup>

The development of oxygen-tolerant ATRP techniques has been another significant breakthrough.<sup>19</sup> Traditionally, ATRP required strict oxygen-free conditions to avoid interference with the polymerization process.<sup>20</sup> Even trace amounts of oxygen in Cu-catalyzed ATRP could oxidize the catalyst to its inactive

form. The elimination of the need for time-consuming oxygen removal prior to polymerization has streamlined the process, making ATRP more accessible to non-experts.<sup>11,19,21–23</sup>

Interestingly, the combination of light and water in photoiniferter reversible addition–fragmentation chain transfer (RAFT) polymerization was advantageous for the synthesis of ultra-high molecular weight (UHMW) polymers, which have potential applications in the biomedical (e.g., hydrogel toughening, mechanochromic sensing),<sup>24</sup> marine, and construction sectors.<sup>24–27</sup> Synthesis of such polymers by ATRP required special conditions, including the use of high pressure (HP).<sup>28–32</sup>

When considering the effect of HP on each of the elementary reactions in the polymerization process, it can be stated that: (i) the rate of initiation is slightly reduced by pressure, and the decomposition of thermoinitiators is also retarded by HP; (ii) the rate of propagation is strongly accelerated by HP; (iii) in most cases, HP accelerates chain transfer reactions, though the effect is smaller than in propagation; and (iv) in diffusion-controlled processes, the termination is retarded by HP due to the increased system viscosity.<sup>33</sup> On the other hand, utilizing HP in ATRP increases both the propagation rate coefficient ( $k_p$ ) and the ATRP equilibrium constant ( $K_{\text{ATRP}}$ ). It also reduces bimolecular termination ( $k_t$ ) in a diffusion-controlled process.<sup>28–31</sup> Moreover, HP affects the propagation–depropagation equilibrium during polymerizations with reversible deactivation, raising the ceiling temperature ( $T_c$ ) and enhancing the polymerizability of several monomers.<sup>34–38</sup> To set the scene properly, it is important to mention the pioneering works concerning HP-ATRP by the teams of Fukuda,<sup>39</sup> Buback,<sup>28–31</sup> and Matyjaszewski.<sup>30–32,40,41</sup> As reported, HP-ATRP strategies allowed UHMWP of up to approximately 2 500 000 to be obtained.<sup>39</sup> Herein, we have developed a visible-light-mediated ATRP under HP for water-soluble UHMW polymer synthesis without deoxygenation of the reaction mixture. Although high pressure combined with light irradiation (HP&LI) has been successfully implemented in organocatalyzed ATRP and photo-induced free radical polymerization (FRP),<sup>36</sup> its role in UHMW polymer synthesis in water remains unexplored.

<sup>a</sup> Institute of Physics, University of Silesia, 75 Pulku Piechoty 1, 41-500 Chorzów, Poland

<sup>b</sup> Silesian Center of Education and Interdisciplinary Research, University of Silesia, 75 Pulku Piechoty 1A, 41-500 Chorzów, Poland.  
E-mail: paulina.maksym@us.edu.pl

<sup>c</sup> Department of Pharmacognosy and Phytochemistry, Faculty of Pharmaceutical Sciences in Sosnowiec, Medical University of Silesia in Katowice, Jagiellońska 4, 41-200 Sosnowiec, Poland

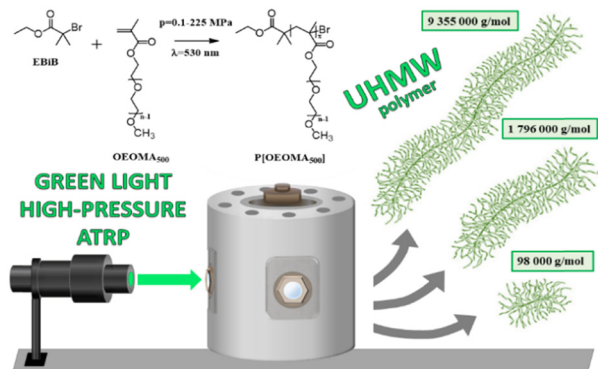
<sup>d</sup> Department of Chemistry, Carnegie Mellon University, 4400 Fifth Avenue, Pittsburgh, PA 15213, USA. E-mail: km3b@andrew.cmu.edu

<sup>e</sup> Faculty of Chemistry, University of Warsaw, Pasteura 1, 02-093 Warsaw, Poland

<sup>f</sup> Institute of Materials Engineering, University of Silesia, 75 Pulku Piechoty 1A, 41-500 Chorzów, Poland

† Electronic supplementary information (ESI) available. See DOI: <https://doi.org/10.1039/d3cc04982e>





Scheme 1 Synthetic outline for OEOMA<sub>500</sub> HP&LI ATRP.

Driven by recent achievements in photoinduced ATRP<sup>11,42,43</sup> we decided to investigate photoredox/copper dual catalysis under HP. Applying pressures of up to 225 MPa and green light irradiation (LL,  $\lambda = 530$  nm), resulted in polymers with molecular weights of up to 9 350 000 and relatively low dispersity values ( $D < 1.49$ ) (Scheme 1). We optimized the conditions for the photoredox/Cu-catalyzed ATRP at different pressure values (Table 1) using oligo(ethylene glycol) methyl ether methacrylate (average  $M_n = 500$ , OEOMA<sub>500</sub>) as the model macromonomer, ethyl  $\alpha$ -bromoisobutyrate (EBiB) as the initiator, eosin Y dye (EYH<sub>2</sub>) as the photocatalyst and CuBr<sub>2</sub>/TPMA (TPMA = tris(2-pyridylmethyl)amine) as the deactivator, with water/DMSO and phosphate-buffered saline (PBS) as a solvent mixture. The experiments were performed in quartz capsules, sealed at both ends with Teflon caps without deoxygenation of the reaction mixture. All experiments were conducted at 750 rpm and 298.15 K, with a constant distance of 5 cm between the light source and the HP chamber's sapphire window (see ESI,† Fig. S1). <sup>1</sup>H NMR and <sup>13</sup>C NMR spectra of the synthesized P[OEOMA<sub>500</sub>] are presented in ESI,† Fig. S2.

Initially, the ATRP was performed in the following molar ratios: [OEOMA<sub>500</sub>]<sub>0</sub>/[EBiB]<sub>0</sub>/[EYH<sub>2</sub>]<sub>0</sub>/[CuBr<sub>2</sub>]<sub>0</sub>/[TPMA]<sub>0</sub> = 200/1/0.005/0.2/0.6 at a pressure of 0.1 MPa (Table 1, entry 1). After 30 min of green light irradiation, >99% monomer conversion was observed by <sup>1</sup>H NMR. However, size exclusion chromatography with a low-angle light scattering detector (SEC-LALLS) revealed that the polymer had a moderate dispersity ( $D$ ) of 1.44. This could be attributed to the excessive reduction of the [Br–Cu<sup>II</sup>/L]<sup>+</sup> by excited eosin Y, leading to a high concentration

of radicals and a loss of control over the polymerization process. To overcome this, the concentration of EYH<sub>2</sub> was reduced by half, resulting in a polymer with a nearly perfect match between the theoretical and the absolute molecular weight (100 000 vs. 98 000), along with a low dispersity of 1.11 (Table 1, entry 2). Next, we investigated the effect of HP (125 MPa) on the polymerization process using molar ratios of [OEOMA<sub>500</sub>]<sub>0</sub>/[EBiB]<sub>0</sub>/[EYH<sub>2</sub>]<sub>0</sub>/[CuBr<sub>2</sub>]<sub>0</sub>/[TPMA]<sub>0</sub> = 1000/1/0.0025/1/3 (Table 1, entry 3). After 1 h, the monomer conversion was only 18% and the ATRP exhibited uncontrolled behavior, resulting in a polymer with high dispersity ( $D = 1.75$ ). Presumably, HP shifted the ATRP equilibrium too much toward radical formation, leading to excessive radical termination. Further experiments were carried out to determine the optimal DMSO concentration at 125 MPa (Table 1, entries 4–6). The best result was achieved with 30% DMSO since well-defined P(OEOMA<sub>500</sub>) with a narrow molecular weight distribution of 1.19 and a molecular weight of 193 300 was obtained (Table 1, entry 4). For comparison, the polymer obtained at 10% DMSO had a dispersity of 1.75 (Table 1, entry 3), while at 50% (Table 1, entry 6) the dispersity was lower but still relatively high ( $D = 1.58$ ). Reducing the TPMA ligand concentration ([CuBr<sub>2</sub>]<sub>0</sub>/[TPMA]<sub>0</sub> = 1/1.5) provided optimal results, allowing polymers with a good agreement between theoretical ( $M_{n,th}$ ) and absolute molecular weights ( $M_{n,LALLS}$ ) and dispersities between 1.18 and 1.34 (Table 1) to be obtained. Adjusting the DMSO concentration was also crucial to achieve better control over the polymerization, since increased pressure might lead to the crystallization of the OEOMA<sub>500</sub> macromonomer<sup>44</sup> or the resulting polymer in water, hindering the polymerization process. Also, a small amount of DMSO is needed to trap singlet oxygen, as was demonstrated in the very recent work of Matyjaszewski's team.<sup>45</sup>

To gain a deeper insight into the polymerization process under HP&LI, we studied its kinetics. As shown in Fig. 1, the experimental data fit linear semilogarithmic plots. Using HP (225 MPa) significantly accelerated the polymerization rate, reaching 56% monomer conversion within just one hour – equivalent to results at 0.1 MPa after 69 hours. This emphasizes the significant effect of the HP on the polymerization rate. Kinetic studies indicated slow initiation at pressures of 150 MPa and 175 MPa (see ESI,† Fig. S3 and S4). For a more comprehensive view of the effect of pressure on the HP&LI-ATRP, we conducted kinetic calculations. We employed a plot of the logarithm of the

Table 1 Optimization of photoredox/Cu-catalyzed ATRP of OEOMA<sub>500</sub> under HP<sup>a</sup>

No	[OEOMA <sub>500</sub> ] <sub>0</sub> /[EBiB] <sub>0</sub> /[EYH <sub>2</sub> ] <sub>0</sub> /[CuBr <sub>2</sub> ] <sub>0</sub> /[TPMA] <sub>0</sub>	DMSO v/v [%]	Time [h]	$P$ [MPa]	Conv. [%] <sup>a</sup>	DP <sup>b</sup>	$M_{n,th}$ <sup>b</sup>	$M_{n,LALLS}$ <sup>c</sup>	$D^c$
1	200/1/0.005/0.2/0.6	10	0.5	0.1	> 99	200	100 000	51 100	1.44
2	200/1/0.0025/0.2/0.6	10	0.5	0.1	> 99	200	100 000	98 000	1.11
3	1000/1/0.0025/1/3	10	1	125	18	180	90 000	194 000	1.75
4	1000/1/0.0025/1/3	30	1	125	46	460	230 000	193 300	1.19
5	1000/1/0.0025/1/3	30	1	0.1	28	280	140 000	156 100	1.30
6	1000/1/0.0025/1/3	50	1	125	95	950	475 000	409 500	1.58
7	1000/1/0.0025/1/1.5	30	1	75	12	120	60 000	59 100	1.10
8	1000/1/0.0025/1/1.5	30	0.5	150	35	350	175 000	106 200	1.20

<sup>a</sup> Reaction conditions: [OEOMA<sub>500</sub>]<sub>0</sub>/[EBiB]<sub>0</sub>/[EYH<sub>2</sub>]<sub>0</sub>/[CuBr<sub>2</sub>]<sub>0</sub>/[TPMA]<sub>0</sub> =  $x/1/x/x/x$ , [OEOMA<sub>500</sub>] = 300 mM, in PBS with DMSO. <sup>b</sup> Determined by <sup>1</sup>H NMR spectroscopy. <sup>c</sup> Determined by SEC-LALLS (DMF with LiBr as an eluent).



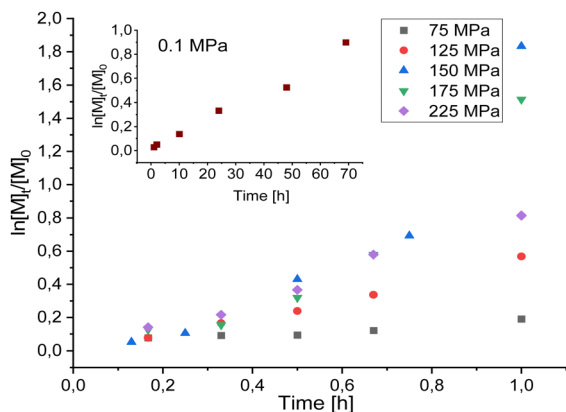


Fig. 1 The semilogarithmic kinetic plots as a function of time for HP&LI ATRP of OEOMA<sub>500</sub> under different pressures.

apparent polymerization rate as a function of pressure, expressed by eqn (1):

$$R_p = -\frac{d \ln[M]}{dt} = k_p[P^*] = k_p K_{ATRP} \frac{[Cu^I][P-Br]}{[Cu^{II}]}, \quad (1)$$

where  $[P^*]$  represents the concentration of propagating free radicals,  $[M]$  is the monomer concentration, and  $k_p$  is the propagation rate coefficient. The  $k_p$  values were derived from the slopes of the semilogarithmic kinetic plots in the linear region of each pressure value (see ESI†). Interestingly, HP increased the polymerization rate up to a certain limit ( $p = 150$  MPa).

Further increase in pressure could lead to inhomogeneity and a potential loss of transparency, which may perturb photo ATRP. We observed that beyond a pressure of 150 MPa, the ATRP rate gradually decreased in the 175–225 MPa range. The reduced rate at pressures higher than 150 MPa is likely due to physical effects, such as increased viscosity or inhomogeneity of the polymerization mixture. This observation aligns with previous results of RAFT and FRP polymerizations of other sterically hindered monomers.<sup>35</sup>

Next, we extracted information about the apparent reaction volume  $\Delta V_R$  from the plot of  $\ln K_{ATRP}$  as a function of pressure (see ESI†, Fig. S5), which was found to be  $-73.60 \pm 3.00 \text{ cm}^3 \text{ mol}^{-1}$ . The slope of the linear  $\ln K_{ATRP}$  vs.  $p$  correlation yields a reaction volume according to eqn 2:

$$\left( \frac{\partial \ln K_{ATRP}}{\partial p} \right)_T = -\frac{\Delta V_R}{RT}, \quad (2)$$

where  $R$  is the gas constant.

The large  $\Delta V_R$  shows that pressure can effectively adjust the ATRP equilibrium constants. Notably, Buback *et al.* extensively investigated the influence of pressure on ATRP equilibrium constants during Cu-mediated polymerization of various monomers, including styrene,<sup>29,31</sup> methyl methacrylate,<sup>30,40</sup> or *n*-butyl acrylate.<sup>41</sup> They found that the initiator type had a minimal effect on  $K_{ATRP}$ , while the ligand type had the most significant impact. The largest negative  $\Delta V_R$  values, determined from  $K_{ATRP}$ , reaching  $\Delta V_R = -33 \text{ cm}^3 \text{ mol}^{-1}$ , they observed in systems using the Me<sub>6</sub>TREN ligand and acetonitrile as the solvent.<sup>28,30,31</sup> The  $\Delta V_R$  value determined in our studies is considerably lower, possibly due to the solvent used. Notably, water's interactions with active and dormant species may alter their volume transitions. Also, intermolecular interactions in water, like hydrogen bonding, can cause distinct volume changes during polymerization compared to organic solvents.<sup>42,46–48</sup>

Additionally, polymers obtained in water have a higher MW, and heat dissipation during polymerization is more efficient.<sup>47</sup> Next, the photoredox/Cu-catalyzed ATRP was used to synthesize UHMW polymers with target degrees of polymerization of 10 000 (Table 2, entry 1) and 30 000 (Table 2, entry 2) at pressures of 150 MPa and 175 MPa, respectively. After 20 h, a polymer with  $M_{n,LALLS} = 1\,796\,000$  was obtained with a moderate dispersity of 1.47. The application of 175 MPa pressure resulted in polymers with a molecular weight of 9 355 000 ( $M_{n,th} = 9\,750\,000$ ) and a dispersity of 1.46 after 48 hours (Table 2, entry 3). We also investigated the effect of initiator type on the ATRP process by comparing EBiB with HOBiB (2-hydroxyethyl 2-bromoisobutyrate). The resulting polymers had similar parameters:  $M_{n,LALLS} = 1\,807\,000$ ,  $D = 1.39$  for HOBiB (Table 2, entry 3), and  $M_{n,LALLS} = 1\,796\,000$ ,  $D = 1.41$  for EBiB (Table 2, entry 1). The monomer conversion was slightly higher (by 8%) when the HOBiB initiator was used. The selected SEC traces of P(OEOMA<sub>500</sub>) synthesized under different conditions are shown in Fig. S6 and S7a in the ESI†. As shown in Fig. S7a (ESI†), for the polymer with molar mass above 9 million Da, a tailing at the low MW fraction is noticeable. To confirm the chain-end fidelity, a chain extension experiment was performed with OEOMA<sub>500</sub> (see Table S1, Fig. S7b and S8, ESI†). After 6 hours of green light irradiation at a pressure of 150 MPa, we observed full monomer conversion and the resulting copolymer increased the MW from 33 700 to 1 234 300 and the dispersity was 1.29.

The research was further extended to include the polymerization of 2-hydroxyethyl acrylate (HEA) using TPMA and Me<sub>6</sub>TREN ligands, in order to test the versatility of our methodology. Detailed results can be found in the ESI†, specifically in Table S2 and Fig. S9 and S10 (ESI†). In summary, we

Table 2 Synthesis of UHMW polymers under HP&LI<sup>a</sup>

No	[OEOMA <sub>500</sub> ] <sub>0</sub> /[EBiB] <sub>0</sub> /[EYH <sub>2</sub> ] <sub>0</sub> /[CuBr <sub>2</sub> ] <sub>0</sub> /[TPMA] <sub>0</sub>	DMSO v/v [%]	Time [h]	<i>P</i> [MPa]	Conv. [%] <sup>a</sup>	DP <sup>b</sup>	<i>M</i> <sub>n,th</sub> <sup>b</sup>	<i>M</i> <sub>n,LALLS</sub> <sup>c</sup>	<i>D</i> <sup>c</sup>
1	10 000/1/0.0025/1/1.5	30	24	150	20	2000	1 000 000	1 796 000	1.41
2	30 000/1/0.0025/1/1.5	30	48	175	65	19 500	9 750 000	9 355 000	1.46
3*	10 000/1/0.0025/1/1.5	30	24	150	28	2800	1 400 000	1 807 000	1.39

<sup>a</sup> Reaction conditions: [OEOMA<sub>500</sub>]<sub>0</sub>/[EBiB]<sub>0</sub>/[EYH<sub>2</sub>]<sub>0</sub>/[CuBr<sub>2</sub>]<sub>0</sub>/[TPMA]<sub>0</sub> = *x*/1/*x*/*x*/*x*, [OEOMA<sub>500</sub>] = 300 mM, in PBS with DMSO. <sup>b</sup> Determined by <sup>1</sup>H NMR spectroscopy. <sup>c</sup> Determined by SEC-LALLS (DMF with LiBr as an eluent). \*HOBiB as the initiator.



synthesized well-defined polymers in a wide range of MWs reaching up to 1 134 000. Additionally, for UHMWP, higher *D* values were noted, which was consistent with the findings from previous scientific reports.<sup>49,50</sup>

In conclusion, we have developed a new approach that combines photoredox/copper dual catalysis with high pressure to synthesize UHMW poly(methacrylates) and poly(acrylates) with molecular weights reaching up to *ca.* 10 million, previously unattainable by ATRP techniques. Our study has also revealed the relationship between pressure, polymerization rate, concentration of catalyst and type of solvent, providing valuable insights into the intricate interplay between these factors.

P. M. and R. B. are thankful for financial support from the Polish National Science Centre within the SONATA project (DEC-2018/31/D/ST5/03464). R. B. is grateful for financial support from the Foundation for Polish Science within the START project. K. M. and G. S. acknowledge support from NSF (CHE 2000391). G. S. gratefully acknowledges the Polish National Agency for Academic Exchange (BPN/PPO/2022/1/00027) for financial support.

## Conflicts of interest

There are no conflicts to declare.

## References

- 1 J. S. Wang and K. Matyjaszewski, *J. Am. Chem. Soc.*, 1995, **117**, 5614–5615.
- 2 K. Parkatzidis, H. S. Wang, N. P. Truong and A. Anastasaki, *Chem.*, 2020, **6**, 1575–1588.
- 3 F. Lorandi, M. Fantin and K. Matyjaszewski, *J. Am. Chem. Soc.*, 2022, **144**, 15413–15430.
- 4 N. Corrigan, K. Jung, G. Moad, C. J. Hawker, K. Matyjaszewski and C. Boyer, *Prog. Polym. Sci.*, 2020, **111**, 101311.
- 5 T. G. Ribelli, F. Lorandi, M. Fantin and K. Matyjaszewski, *Macromol. Rapid Commun.*, 2019, **40**, 1800616.
- 6 M. Chen, M. Zhong and J. A. Johnson, *Chem. Rev.*, 2016, **116**, 10167–10211.
- 7 X. Pan, M. A. Tasdelen, J. Laun, T. Junkers, Y. Yagci and K. Matyjaszewski, *Prog. Polym. Sci.*, 2016, **62**, 73–125.
- 8 D. Konkolewicz, K. Schröder, J. Buback, S. Bernhard and K. Matyjaszewski, *ACS Macro Lett.*, 2012, **1**, 1219–1223.
- 9 T. G. Ribelli, D. Konkolewicz, S. Bernhard and K. Matyjaszewski, *J. Am. Chem. Soc.*, 2014, **136**, 13303–13312.
- 10 C. Wu, N. Corrigan, C. H. Lim, W. Liu, G. Miyake and C. Boyer, *Chem. Rev.*, 2022, **122**, 5476–5518.
- 11 G. Szczepaniak, J. Jeong, K. Kapil, S. Dadashi-Silab, S. S. Yerneni, P. Ratajczyk, S. Lathwal, D. J. Schild, S. R. Das and K. Matyjaszewski, *Chem. Sci.*, 2022, **13**, 11540–11550.
- 12 M. Fantin, A. A. Isse, A. Gennaro and K. Matyjaszewski, *Macromolecules*, 2015, **48**, 6862–6875.
- 13 S. Averick, A. Simakova, S. Park, D. Konkolewicz, A. J. D. Magenau, R. A. Mehl and K. Matyjaszewski, *ACS Macro Lett.*, 2012, **1**, 6–10.
- 14 S. Dworakowska, F. Lorandi, A. Gorczyński and K. Matyjaszewski, *Adv. Sci.*, 2022, **9**, 2106076.
- 15 G. R. Jones, A. Anastasaki, R. Whitfield, N. Engeli, E. Liarou and D. M. Haddleton, *Angew. Chem., Int. Ed.*, 2018, **57**, 10468–10482.
- 16 S. L. Baker, B. Kaupbayeva, S. Lathwal, S. R. Das, A. J. Russell and K. Matyjaszewski, *Biomacromolecules*, 2019, **20**, 4272–4298.
- 17 C. Chen, D. Y. W. Ng and T. Weil, *Prog. Polym. Sci.*, 2020, **105**, 101241.
- 18 J. Jeong, X. Hu, H. Murata, G. Szczepaniak, M. Rachwalak, A. Kietrys, S. R. Das and K. Matyjaszewski, *J. Am. Chem. Soc.*, 2023, **145**, 14435–14445.
- 19 G. Szczepaniak, L. Fu, H. Jafari, K. Kapil and K. Matyjaszewski, *Acc. Chem. Res.*, 2021, **54**, 1779–1790.
- 20 M. Schmal, *React. Chem. Eng.*, 2020, **8**, 119–130.
- 21 J. Yeow, R. Chapman, A. J. Gormley and C. Boyer, *Chem. Soc. Rev.*, 2018, **47**, 4357–4387.
- 22 A. E. Enciso, L. Fu, A. J. Russell and K. Matyjaszewski, *Angew. Chem., Int. Ed.*, 2018, **57**, 933–936.
- 23 G. Szczepaniak, M. Łagodzińska, S. Dadashi-Silab, A. Gorczyński and K. Matyjaszewski, *Chem. Sci.*, 2020, **11**, 8809–8816.
- 24 R. N. Carmean, M. B. Sims, C. A. Figg, P. J. Hurst, J. P. Patterson and B. S. Sumerlin, *ACS Macro Lett.*, 2020, **9**, 613–618.
- 25 R. N. Carmean, T. E. Becker, M. B. Sims and B. S. Sumerlin, *Chem.*, 2017, **2**, 93–101.
- 26 M. Kamigaito and K. Satoh, *Chem.*, 2017, **2**, 13–15.
- 27 K. Patel, S. H. Chikkali and S. Sivaram, *Prog. Polym. Sci.*, 2020, **109**, 101290.
- 28 M. Buback and J. Morick, *Macromol. Chem. Phys.*, 2010, **211**, 2154–2161.
- 29 J. Pietrasik, C. M. Hui, W. Chaladaj, H. Dong, J. Choi, J. Jurczak, M. R. Bockstaller and K. Matyjaszewski, *Macromol. Rapid Commun.*, 2011, **32**, 295–301.
- 30 J. Morick, M. Buback and K. Matyjaszewski, *Macromol. Chem. Phys.*, 2012, **213**, 2287–2292.
- 31 J. Morick, M. Buback and K. Matyjaszewski, *Macromol. Chem. Phys.*, 2011, **212**, 2423–2428.
- 32 P. Kwiatkowski, J. Jurczak, J. Pietrasik, W. Jakubowski, L. Mueller and K. Matyjaszewski, *Macromolecules*, 2008, **41**, 1067–1069.
- 33 N. L. Zutty and R. D. Burkhart, in *Polymerization and polycondensation processes*, ed. N. A. J. Platzer, American Chemical Society, 1962, ch. 3, vol. 34, pp. 52–59.
- 34 J. Rzaev and J. Penelle, *Macromolecules*, 2002, **35**, 1489–1490.
- 35 P. Maksym, M. Tarnacka, A. Dzienia, K. Wolnica, M. Dulski, K. Erfurt, A. Chrobok, A. Zięba, A. Brzózka, G. Sulka, R. Bielas, K. Kaminski and M. Paluch, *RSC Adv.*, 2019, **9**, 6396–6408.
- 36 P. Maksym, M. Tarnacka, R. Bernat, A. Dzienia, A. Szelwicka, B. Hachuła, A. Chrobok, M. Paluch and K. Kamiński, *Polym. Chem.*, 2021, **12**, 4418–4427.
- 37 P. Maksym, M. Tarnacka, A. Dzienia, K. Erfurt, A. Brzeczek-Szafran, A. Chrobok, A. Zięba, K. Kaminski and M. Paluch, *Polymer*, 2018, **140**, 158–166.
- 38 P. Maksym, M. Tarnacka, R. Bernat, R. Bielas, A. Mielańczyk, B. Hachuła, K. Kaminski and M. Paluch, *J. Polym. Sci.*, 2020, **58**, 1393–1399.
- 39 T. Arita, Y. Kayama, K. Ohno, Y. Tsujii and T. Fukuda, *Polymer*, 2008, **49**, 2426–2429.
- 40 H. Schroeder, M. Buback and K. Matyjaszewski, *Macromol. Chem. Phys.*, 2014, **215**, 44–53.
- 41 Y. Wang, H. Schroeder, J. Morick, M. Buback and K. Matyjaszewski, *Macromol. Rapid Commun.*, 2013, **34**, 604–609.
- 42 K. Kapil, A. M. Jazani, G. Szczepaniak, H. Murata, M. Olszewski and K. Matyjaszewski, *Macromolecules*, 2023, **56**, 2017–2026.
- 43 K. Kapil, G. Szczepaniak, M. R. Martinez, H. Murata, A. M. Jazani, J. Jeong, S. R. Das and K. Matyjaszewski, *Angew. Chem., Int. Ed.*, 2023, **62**, e202217658.
- 44 A. Czaderna-Lekka, K. Piechocki, M. Kozanecki and L. Okrasa, *J. Phys. Chem. Solids*, 2020, **140**, 109359.
- 45 X. Hu, G. Szczepaniak, A. Lewandowska-Andralojc, J. Jeong, B. Li, H. Murata, R. Yin, A. M. Jazani, S. R. Das and K. Matyjaszewski, *J. Am. Chem. Soc.*, 2023, **145**, 24315–24327.
- 46 M. Fantin, A. A. Isse, K. Matyjaszewski and A. Gennaro, *Macromolecules*, 2017, **50**, 2696–2705.
- 47 M. Buback, R. A. Hutchinson and I. Lacić, *Prog. Polym. Sci.*, 2023, **138**, 101645.
- 48 S. Smolne, S. Weber and M. Buback, *Macromol. Chem. Phys.*, 2016, **217**, 2391–2401.
- 49 J. Collins, T. G. McKenzie, M. D. Nothling, M. Ashokkumar and G. Qiao, *Polym. Chem.*, 2018, **9**, 2562–2568.
- 50 X. Leng, N. H. Nguyen, B. van Beusekom, D. A. Wilson and V. Percec, *Polym. Chem.*, 2013, **4**, 2995–3004.

